Fuel Processing Technology 157 (2017) 1–11

Contents lists available at ScienceDirect

Fuel Processing Technology

journal homepage: www.elsevier.com/locate/fuproc

Research article

Characterising pulverised fuel ignition in a visual drop tube furnace by use of a high-speed imaging technique

Archi C. Sarroza, Tom D. Bennet, Carol Eastwick, Hao Liu *

Faculty of Engineering, University of Nottingham, University Park, Nottingham NG7 2RD, United Kingdom

ARTICLE INFO

Article history:
Received 13 August 2016
Received in revised form 1 November 2016
Accepted 4 November 2016
Available online xxxx

Keywords:
Pulverised fuel particle
Ignition distance
Combustion image analysis
Visual drop tube furnace
Biomass co-firing with coal

ABSTRACT

This study investigates the ignition characteristics of pulverised coal, biomass and co-firing by use of a visual drop tube furnace (VDTF) and a high speed imaging technique. Three coals (anthracite, a bituminous coal and a lignite), four biomasses (Pine, Eucalyptus, Olive Residue and Miscanthus) and various biomass-coal mixtures were tested. With each coal, biomass or their mixture, a distinct flame was established within the VDTF through the continuous feeding of the fuel under the environment of air and at a furnace temperature of 800 °C. To observe the ignition point, a Phantom v12.1 high-speed camera was used to capture the videos of fuel combustion at 500 frames per second (FPS). A technique was developed using MATLAB's image analysis tool to automate the ignition point detection. The results of the image processing were used to statistically analyse and determine the changes to the ignition behaviour with different fuels and co-firing ratios.

The results obtained with the tested coals have shown that the distance to ignition increases as the coal volatile matter content decreases, whereas the opposite trend was found for the biomass fuels. Further, the addition of biomass to the anthracite significantly reduces the distance to ignition but a much less pronounced effect on the ignition was found when biomass was co-fired with the bituminous coal or lignite. The synergistic effect on the ignition of biomass-anthracite mixture is mainly attributed to the high volatile content and the potential effects of catalysis from the alkali metals present in the biomass. The results of this study have shown that the VDTF testing coupled with the image analysis technique allows for an effective and simple method of characterising ignition behaviours of pulverised coal, biomass and their mixtures.

1. Introduction

Visualising combustion using imaging techniques is a simple non-intrusive method that can reveal combustion characteristics of individual pulverised fuel (PF) particles and PF burner flames [1,2]. This is usually realised by recording the combustion events occurring in a transparent furnace or through the transparent observation windows of a non-transparent furnace using a high frame rate video camera [2,3,4]. Post-processing and statistically analysing the captured images can determine the ignition behaviours of pulverised fuel particles, flame size, shape and stability. The use of transparent furnaces to observe particle ignition/combustion is not new as there are a number of previous publications in this field [1–3,5], however, image capture is not limited to this type of set-up as imaging techniques encompass a variety of applications - from laboratory scale single particle tests [6], to plant-scale flame observation [4,7–9]. Levendis et al. [2] used high speed imaging techniques to observe single particle combustion for coal and sugarcane-bagasse using a drop tube furnace with a viewing window. Their results specifically demonstrated the technical feasibility of high speed video capture in a combustion environment. A similar study by Zhang et al. [3] focused on measuring the change in combusting particle velocity as it travelled through the furnace. As with the study of Levendis et al. [2], a standing flame was not generated in the test conditions of Zhang et al. [3]. González-Cencerrado et al. [9] successfully used high-speed imaging to characterise the flame behaviours of a 500 kW_{th} swirl burner co-firing coal and biomass in terms of flame brightness, fluctuation amplitude, distribution symmetry, and oscillation frequency. Matthes et al. [4] demonstrated the on-line measurement capability of a high-speed camera set-up in a standing flame environment with a 1 MW_{th} multi-fuel swirl burner. Molcan et al. [8] characterised biomass and coal combustion using a 3 MW_{th} test facility equipped with a low-NOx burner. An optical probe was positioned adjacent to the low-NOx burner to measure the flame temperature profile using two-colour pyrometry. Although a standing flame was observed in [4,8,9], the relative magnitude of the set-up incurred significant testing time and cost. Thus, it would greatly reduce cost and save time if the study on the flame/combustion behaviours of PF fuels, whether coal, biomass or their mixtures, is carried out with a laboratory-scale furnace that can produce a propagating flame without the use of a burner. In addition, literature

* Corresponding author.
E-mail address: liu.hao@nottingham.ac.uk (H. Liu).

http://dx.doi.org/10.1016/j.fuproc.2016.11.002

survey has confirmed that high-speed imaging techniques have rarely been applied to the study of a distinct flame established through the continuous fuel feed without the use of a burner on a laboratory scale furnace such as a drop tube furnace which has been widely used for the ignition studies of PF particles [1,2,5]. A study by Levendis et al. [10] in 1998 already demonstrated the feasibility of such a set-up to observe combustion using high-speed cinematography.

Co-firing has become increasingly prevalent in power plants as a means to introduce biomass into the fuel mix, and plant operators can receive financial subsidies for doing so, without the higher capital investment of undertaking a full conversion to burn biomass exclusively. In being able to predict the ignition of fuel blends, plant operators could envisage the risks of mill fires when the fuels are co-milled, and on flame stability and potential 'blow-back' for safe boiler operation [7,11]. A study by van de Kamp and Morgan [12] highlighted the trade-offs that needed to be considered when choosing a co-firing fuel and the mixture ratio with coal. Although the study was carried out in 1990′s, the core issues identified such as grindability, slagging, fouling and emission trade-offs are still relevant to the current co-firing practices in power plants. Based on the findings in literature [13], it was hypothesised that the distance to ignition, or stand-off distance, would not correlate directly to the proportion of each fuel that was mixed, in so-called 'additive' behaviour. Rather, a more complex synergistic interaction would occur where, for example, a small addition of biomass to coal would cause a disproportionately large reduction in distance to ignition.

Predicting the ignition behaviour of co-firing fuels is not simple, as has been found with investigations on the combustion and ignition of blended coals [7,8,14]. Coals with the same proximate analysis may not necessarily have the same ignition and flame stability characteristics because the ignition depends on early heat release and not on early volatile release [7]. Co-firing on the other hand can result in a shift of the ignition and burnout to lower temperature regions due to the rapid evolution of volatiles from biomass [15]. Moon et al. [15] found that an addition of 10% biomass (blending ratio based on weight) to a low-rank sub-bituminous coal resulted in a significantly enhanced ignition reactivity of the low rank coal. Therefore, the change in the ignition behaviour when blending biomass and coal can be related to two possible causes: either the change is due to the biomass volatile release and ignition triggering the coal to ignite at a lower temperature [15], and/or by relating to the role of alkali metals in the biomass ash, which can catalyse the combustion process [16].

This paper describes how the Visual Drop Tube Furnace (VDTF) was utilised to characterise the ignition and combustion behaviours of biomass and coal, both individually and in various 'co-firing' combinations. Experiments were conducted using the VDTF system that has two water-cooled probes used for continuous feeding and collection of fuel and ash respectively. Although the quartz glass furnace can only be heated to a maximum temperature of 1050 °C, it allowed for the visual observation of the combustion process through a long quartz viewing window. The captured high-speed videos were post-processed frame-by-frame using MATLAB's image analysis tools to statistically describe ignition point fluctuation. To the best of our knowledge, this particular method of automating ignition point analysis has not been reported in literature, especially in the context of solid fuel combustion flames established by continuous fuel feeding, rather than by a burner, in a laboratory-scale combustion furnace such as a drop tube furnace.

2. Methodology

2.1. Apparatus

2.1.1. Visual drop tube furnace

To observe the particle combustion processes, a Visual Drop Tube Furnace (VDTF) was specially designed and manufactured. The VDTF is a vertically oriented laminar flow reactor consisting of a transparent quartz work tube that has a 50 mm internal diameter, a 5 mm thick wall, and is surrounded by heating elements throughout its heated length (1000 mm) (see Fig. 1 for the photographs of the VDTF setup and Fig. 2 for the VDTF schematic). A long viewing window (560 mm × 30 mm) is located parallel to the work tube orientation and is positioned at the mid-section of the furnace assembly. Pulverised fuel particles were continuously injected at a mass flow rate of 1.2 g/min through a water-cooled feeder probe using air as a carrier gas at 1 L/min. The collector probe was also water cooled to quench the fuel particles after passing the 'hot combustion' zone. Secondary air at 5 L/min was introduced at the top of the furnace, co-axially with the primary air from the gap between the inner wall of the work tube and the external wall of the feeder probe. In addition, the flowrate setting for the vacuum pump was matched to the total inlet gas flow. This flow set-up results in a low Reynolds number throughout the length of the work tube. The laminar flow condition ensures that pulverised fuel particles are entrained by the gas flow and travel in a narrow stream along the centre axis of the

Fig. 1. Visual Drop Tube Furnace with a long viewing window (left) and video capture set-up showing Phantom V12.1 high speed camera with 105 mm Nikon lens (right).

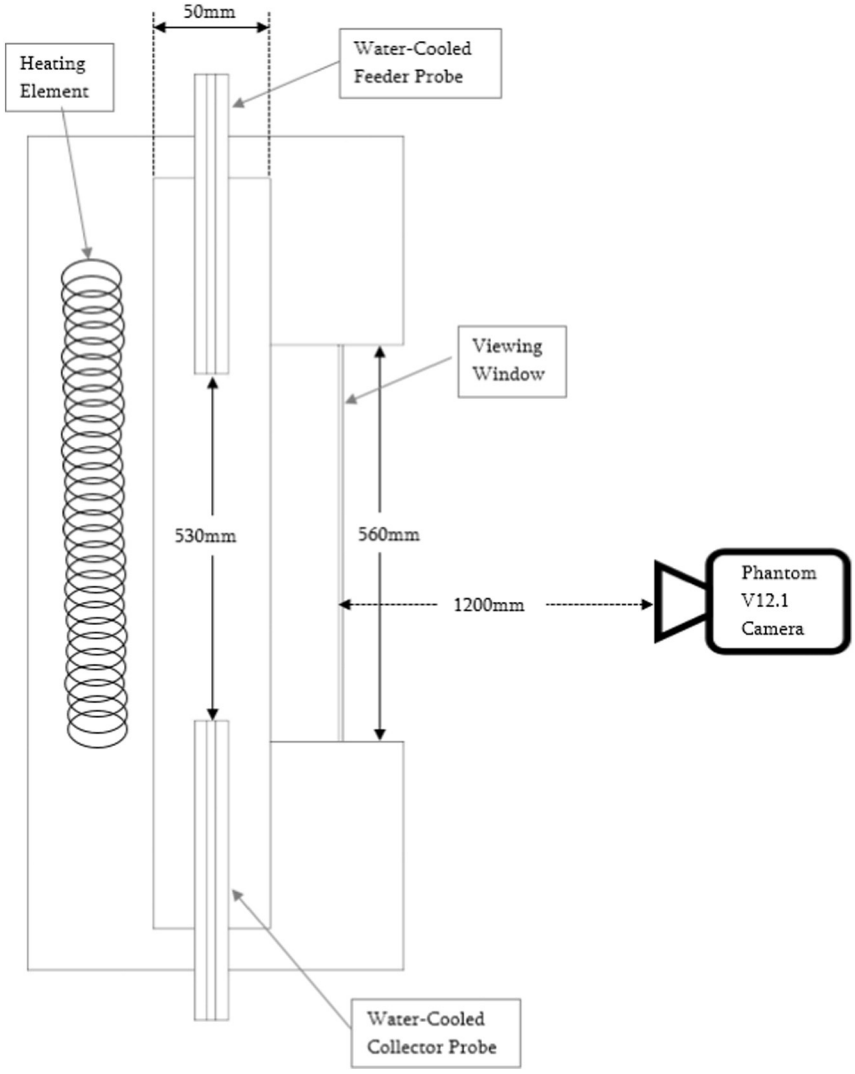

Fig. 2. Schematic of the vertically oriented VDTF: camera is positioned adjacent to the viewing window and tilted at a 90° angle to enable the use of the longer resolution width of the camera sensor. This maximizes the captured area of the required lengthwise 'active' combustion zone.

furnace. The particles are fed via a vibrating plate channel feeder as it provides precise control at low feed rates for solid particles.

The tests described in this paper were carried out at a set furnace temperature of 800 °C with the feeder and collector probes set at a separation distance of 530 mm. The actual reaction temperature between the two probes remained close to the VDTF set temperature at 785 °C with a maximum deviation of ± 5 °C, indicating the fuel combustion zone is close to isothermal.

2.1.2. High speed camera

The ignition point and combustion flame, which can be observed through the quartz window in the furnace, were captured using a Phantom v12.1 high-speed camera (Figs. 1–2). The camera was set to capture the longitudinal 560mmx30mm area of the viewing window with the lens level and adjacent to the ignition point location. The video resolution (width) was minimised where possible by only capturing the window area of the VDTF to reduce image processing time and storage

Table 1
Proximate and ultimate analyses and high heating values (HHV) of the tested fuels.[a]

		Chinacite	El Cerrejon	Lignite	Pine	Eucalyptus	Olive residue	Miscanthus
Proximate analysis	$Moisture_{ar}$	1.3	2.3	8.2	4.4	5.9	6.2	7.1
	$Volatiles_{db}$	8.4	37.5	56.9	83.8	88.3	71.5	68.6
	FC_{db}	86.5	52.5	36.4	15.6	8.7	16.1	23.6
	Ash_{db}	5.1	10.0	6.7	0.6	3.0	12.4	7.8
Ultimate analysis[b] (db wt%)	C	87.7	72.2	62.5	48.0	48.7	45.9	45.2
	H	3.2	4.8	4.8	5.9	5.7	5.7	5.8
	N	1.3	1.5	0.8	0.2	0.2	2.1	1.0
	S	nd	2.4	nd	nd	nd	nd	nd
	O	2.7	9.1	25.2	45.3	42.4	33.9	40.2
HHV (MJ kg^{-1} db)		34.91	29.62	24.77	20.04	20.67	18.39	17.98

[a] Legend: ar = as-received, nd = not detected, db = dry basis, daf = dry ash free.
[b] Oxygen determined by difference.

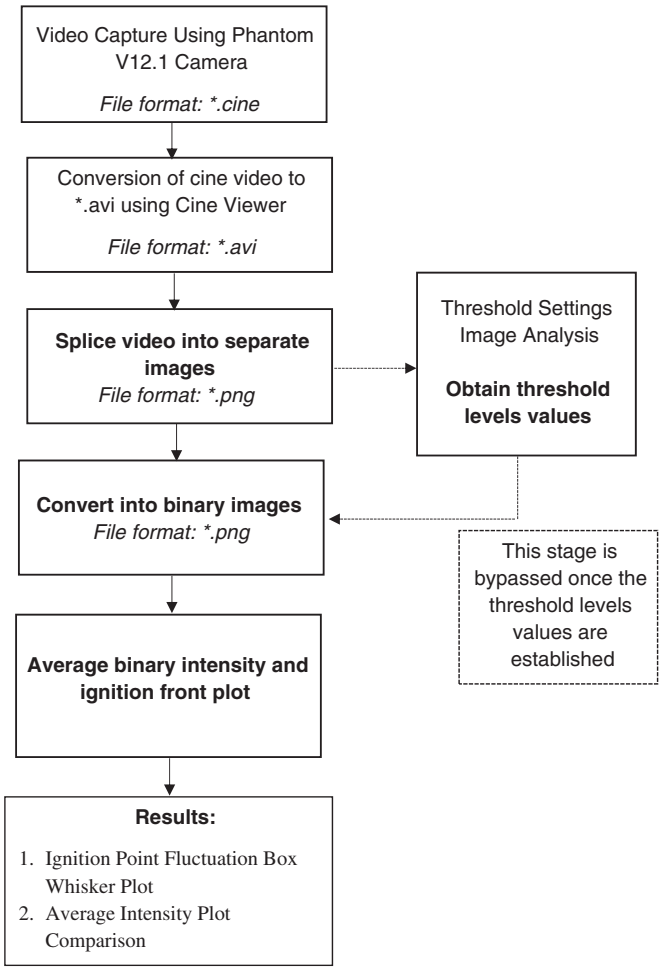

Fig. 3. Diagram of the method used to analyse the captured high speed video from the Phantom v12.1 camera. Steps using MATLAB functions and macros are in bold text while the file formats used for the different stages are in italics.

requirements. A fixed focal length (FFL) 105 mm f/2.8 Nikon lens was used for the ignition point tests because observing the full length of the furnace/flame was of interest. The video was captured at 500 frames per second with a resolution of 1280 × 152 pixels. All video files were stored in a raw grayscale format.

2.2. Fuel preparation

A number of biomass fuels and coals were included in this study to represent the types of fuel used in the UK power generation industry. The proximate and ultimate analyses of these fuels are enumerated in Table 1. The fuels were pulverised using a planetary ball mill before being sieved. A size fraction of 75–106 μm was used for both biomass and coal in the VDTF ignition tests. The narrow range allows for better mixing of the fuels for co-firing tests as well as giving optimal fuel feed flow by the vibrating plate feeder.

2.3. Image analysis

The video file captured by the high-speed Phantom camera is in a *.cine format which is a proprietary file format used by the Phantom Cine Viewer software [17]. An overview of the implemented technique for analysing ignition distance and fluctuation over time is shown in Fig. 3. This highlights all of the MATLAB image post-processing functions and macros used. The primary aim is to convert the cine video files into a useful format that can then be quantitatively analysed. MATLAB was determined to be ideal for image analysis due to available features that can be implemented as automated macro functions. After converting the *.cine files into a *.avi format (built-in conversion tool from Cine Viewer software [17]), a splicing macro is used to extract the video frames into separate image files (*.png format). For the ignition point testing, a sample rate of 500FPS with a resolution of 1280 × 152 pixels was used, which means that for a single second recorded, 500 images can be generated using the splicing macro.

The threshold values of the images are analysed for conversion of the greyscale format (Fig. 4) into a black and white (B&W) image (Fig. 5). The threshold value is used as a base point whereby pixels below the chosen threshold is given a value of 0 = black and the rest of the pixels are given a value of 1 = white. The same threshold value is applied to the rest of the image analysis process as it serves as a base point for the comparison of flame ignition point and flame intensity for the different fuels. This is why the experimental lighting conditions are kept the same along with the camera settings such as exposure time & FPS for all the test cases.

The intensity levels (low & high limits) are manually adjusted until a threshold level is found which filters the glow from the flame. The resulting binary image from Fig. 4b is shown in Fig. 5 and was generated by setting a threshold level of 0.12. This value provided the best threshold level as it reflects the point of ignition clearly whilst at the same time suppressing the "glow" effect around the ignition point. This image was then used as a benchmark to create a macro to automate this process for the rest of the image frames generated from the video. The global image thresholding function in MATLAB that changes grayscale images into a binary format was developed from the method by Otsu [18].

The distilled image is used in evaluating the ignition point as it simplifies pixel variation into two binary values: 1 for white and 0 for black pixels. The levels obtained provide a clear threshold to detect the flame ignition point and at the same time represents the flame intensity. Binary image analysis has been employed in multiple video detection applications. One such example is a study by Chen and Bao [19] whereby

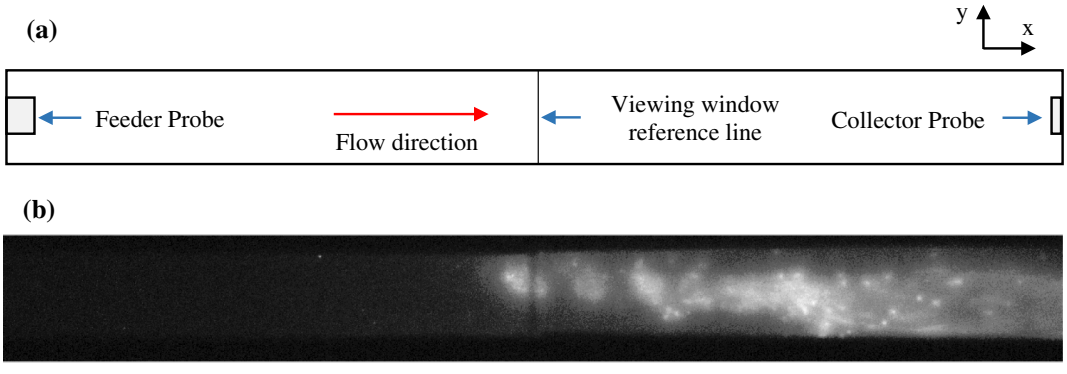

Fig. 4. (a) Schematic showing flow orientation (feeder probe to collector probe) and (b) raw image frame for the combustion of 75–106 μm pine particles.

Fig. 5. Result of converting the grayscale image in Fig. 4b to a binary image using *im2bw* function with a threshold level of 0.12. The image is from the combustion of 75–106 μm pine particles.

frame segmentation techniques were used to individually process and convert images into a binary format. This allows for extracting data such as flame length and amplitude much more easily than that of a grayscale image. It also gives back data such as the size of the flame, which can be determined by the number of white pixels found in a single image frame. The binary image makes the flame edges clearly distinguishable, and it is this property which is then exploited to help define the ignition point of an observed flame.

The ignition point can therefore be quantified by measuring the distance from the feeder edge of the image to the first non-black pixel. This can be done by tracking the pixel intensity value along a line (superimposed on the binary image) through the *improfile* function in MATLAB. The flame front fluctuates both in the axial and radial location with time as the flame was not stabilised on a burner but generated and sustained by the continuous feeding of the fuel particles, and therefore this variation of the flame front needs to be taken into account with the image analysis. Thus, a custom function that allows for integration along the whole width of the image is used. The resulting intensity plot for the binary image in Fig. 5 is shown in Fig. 6 whereby the intensity value lies between the arbitrary value of 0 and 1.

The result obtained from averaging the intensity across the image width is then incorporated into an automated macro which processes the rest of the converted binary images for a specific experimental run. The result for each image is analysed and is then compiled to create a time-averaged binary intensity plot which better reflects the flame characteristics observed from the original high speed footage. This also includes a function to determine distance of the ignition front (in pixels) from the left hand side of the image. The ignition distance is recorded as the first non-zero intensity value. For example in Fig. 6, this is recorded as 600 pixel units from the start of the image (on the x-axis direction). The pixel distance is then converted into mm (0.3 mm per pixel) and is subsequently presented in this format. A pixel measurement tool was used whereby the width of the viewing window gap is used as a basis for calibration for the pixel to mm conversion.

By averaging the results from all of the captured frames, the fluctuation of the flame intensity and the movement of the ignition point are better quantified through a graphical presentation. This also automatically averages out the outliers whereby single white pixels that are observed prematurely and far from the main flame front do not register as a point of ignition.

3. Results and discussion

3.1. Comparison on the ignition distance of different coals

The distance between the feeder probe and the detected point of ignition for the fuels, termed as the distance to ignition, is used as the main characteristic parameter for the ignitibility of the tested fuels in this study. The exact value of the distance to ignition of each fuel will depend on not only the fuel properties but also other test conditions such as the fuel particle size and the furnace temperature. Under the same controlled test conditions, however, the values of the distance to ignition obtained should correctly reflect the ignitibility of the tested fuels. With the selected furnace temperature (800 °C) and the particle size range (75–106 μm), all of the ignition points of the tested coals, biomasses and their mixtures fell within the long viewing window section on the V-DTF and hence enabled all test cases to be video captured with the high-speed camera.

The results on the distance to ignition of the three tested coals are compared using a box plot in Fig. 7. The middle of each box represents the median, the top and bottom of the box represent the third and first quartile, respectively, and the error bars represent the recorded maximum and minimum distances to ignition after anomalies have been excluded. The box plot reflects the fluctuation of the ignition point measurement as discussed in Section 2.3.

Amongst the coals investigated, the ignition distance increases with the Fuel Ratio as expected. Chinacite, an anthracite type of coal, had the least ignitability with the ignition occurring close to the tip of the collector probe and hence the very narrow distribution plot compared to the other fuels being presented. As the lowest rank coal, lignite displayed the highest ignitability amongst the three types of coal samples. In fact its ignition distance is comparable to what was observed with the biomass samples tested in this study (Fig. 8). These VDTF results on the ignition distance are in agreement with the findings of Khatami and Levendis [1] who had observed longer ignition delays for the high

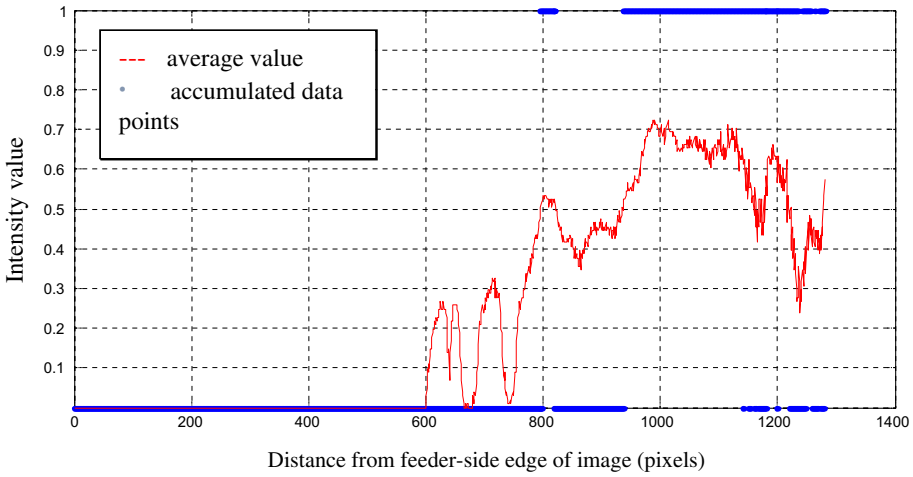

Fig. 6. Single frame averaged intensity plot (along the x-axis) for the binary image in Fig. 5.

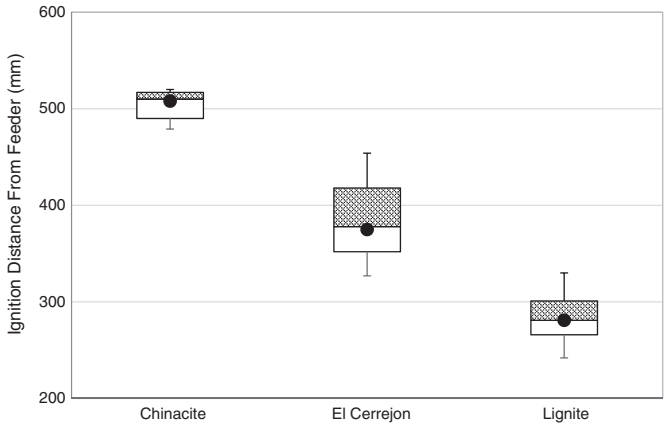

Fig. 7. Distance to ignition of different coals (75–106 μm) at 800 °C furnace temperature. Fuel Ratio (i.e. the ratio between the Fixed Carbon and Volatile Matter) values for the coals presented are as follows: Chinacite = 10.30, El Cerrejon = 1.40, Lignite = 0.64.

rank coals, whilst the low rank coals experienced shorter ignition delays.

3.2. Comparison on the ignition distance of different biomass fuels

Biomass testing was carried out under the same conditions as the coal tests where a particle size range of 75–106 μm was used and the furnace temperature was also set at 800 °C. The high volatile matter content of biomass meant that the ignition would be expected to occur nearer to the point of particle injection. Similar to the coal testing, a box plot is used to show the distances to ignition of the tested biomass fuels (Fig. 8).

Unlike the observations from the coal testing, the distance to ignition for the biomass fuel decreases with the Fuel Ratio. This is further in contrast to previous work by Grotkjaer et al. [20], who asserted that biomass follows the same trend as coal. The inference from [20] was obtained from the correlation results of three types of biomass (straw, poplar wood, and eucalyptus).

The observed ignition/combustion characteristics of the biomass fuels may be attributed to the role of alkali metals present due to their potential of catalysing the combustion process [16,21–23]. In particular, potassium has been previously shown to decrease the peak temperature for volatile combustion [22], and the other major ash elements have also been found to catalyse the reaction and been shown in the following order from the most to the least active [23]:

P>K>Fe>Raw>HCl>Mg>Ca

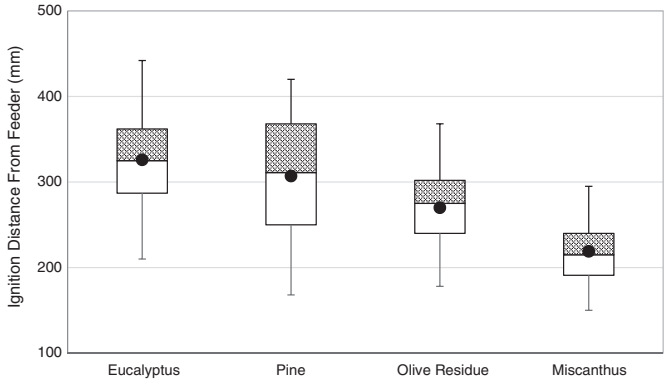

Fig. 8. Distance to ignition with biomass fuel (75–106 μm) at 800 °C furnace temperature. Fuel ratio values for the tested biomass fuels are: Eucalyptus = 0.10, Pine = 0.19, Olive Residue = 0.23, Miscanthus = 0.34.

Table 2
Major ash element content relating to combustion catalysis as measured by X-ray Fluorescence (XRF).

wt% basis	Miscanthus	Olive residue	Pine	Eucalyptus
P_2O_5	3.7	4.64	4.38	1.72
K_2O	17.2	36.5	6.99	6.78
Fe_2O_3	2.4	1.31	1.60	0.82
HCl	nd	3.07	nd	nd
MgO	1.8	8.74	9.94	7.96
CaO	8.3	10.09	35.19	42.15

It can be noted from Table 1 that Olive Residue and Miscanthus have much higher ash contents than Pine and Eucalyptus, whereas Table 2 also shows that Olive Residue and Miscanthus contain higher weight percentages of potassium oxides in their ashes than Eucalyptus and Pine.

The tested biomass fuels were also analysed using TGA under slow heating rate conditions as this allows for the volatiles release of the fuels to be compared under thermally controlled conditions (Fig. 9). The low temperature ramp of 3 °C min^{-1} ensures that the surface is not heating up significantly faster than the particle's core thereby reducing the temperature difference. Olive Residue and Eucalyptus display two distinct devolatilisation peaks which relate to the separate decomposition temperatures of the hemicellulose and cellulose component [24], whilst Miscanthus and Pine have a more prominent single peak. The fuels can be ranked in terms of their main (with the highest wt% $°C^{-1}$) devolatilisation peak temperature, from the highest to the lowest:

Pine ~ Eucalyptus>Olive Residue>Miscanthus

The VDTF test results (Fig. 8) suggest that the biomasses with the lower peak devolatilisation temperatures, i.e. Miscanthus and Olive Residue, had the shorter distances to ignition, whereas the biomasses (Eucalyptus and Pine) which have much higher peak devolatilisation rates actually had longer distances to ignition due to the peak devolatilisation rates being reached at much higher temperatures. This ranking is analogous to the ignition analysis study by Jones et al. [11] which categorised biomass ignitability based on characteristic (peak) temperature and kinetic parameters. Miscanthus ranked higher than Pine with respect to general reactivity and thus was categorised as a high risk to low temperature ignition [11]. The vast magnitude difference in the heating rates between the TGA and VDTF will conceivably contribute to the divergence of the physio-chemical effects on combustion as observed in previous studies [24]. TGA combustion tests at low heating rates have merit in terms of providing indicative ignition behaviours under high heating rates as demonstrated by Li et al. [25]. It is irrefutable, however, that in the VDTF the fuel samples are heated at such a high rate that the point of ignition does not necessarily occur at the point of the peak devolatilisation. The start of ignition would be largely dictated by the diffusion rate of oxygen into the volatile cloud and it is at this stage that ignition is visually observed. It is expected that some of the devolatilised alkali and alkaline earth metals would be involved in catalysing the combustion, resulting in a reduction of the ignition temperature and hence leading to a shorter ignition distance in the VDTF.

3.3. Co-firing analysis

To determine the effects of mixing different fuels on ignition, coal and biomass were blended and co-fired with different energy ratios. The same particle size range (75–106 μm) from both fuels ensured the uniformity of the biomass-coal mixture. It is well documented that particle size affects the particle heating rate and hence the ignition distance. As observed by Weber et al. [26], hard coal which was milled to its typical distribution size (<75um) ignited closer to the burner compared with the biomass fuels which consisted of particles larger than

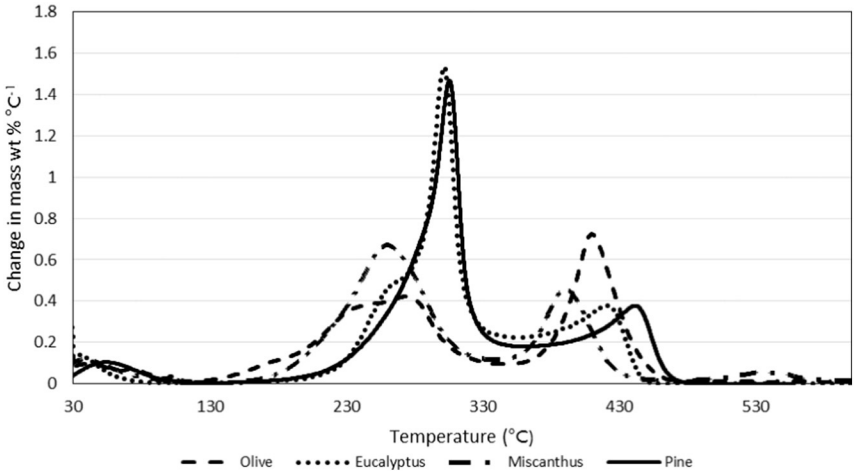

Fig. 9. Rates of weight change of biomass fuels when heated in air at 3 °C min^{-1}.

250 μm. Similar effects of particle sizes on ignition distance had been observed with the present experimental setup with the tested coals and biomass fuels [27]. Both TGA and VDTF tests were carried out to characterise the performance of co-firing the different biomass-coal mixtures.

3.3.1. TGA testing

Fig. 10 shows the TGA combustion rates under slow heating rate conditions (3 °C/min) for Chinacite, Miscanthus and their 50:50 mixture (on fuel energy (HHV) ratio basis), whereas Fig. 11 shows the TGA combustion test results for El Cerrejon, Miscanthus and their 50:50 mixture. The first peak of mass loss for Miscanthus was observed at 250 °C whilst for Chinacite and El Cerrejon these were observed at 475 °C and 450 °C respectively. The second peak of mass loss observed for Miscanthus at 390 °C was the char combustion. Under slow heating rate conditions, the 50:50 biomass to coal co-firing mixture, for both Chinacite (Fig. 10) and El Cerrejon (Fig. 11), shows an additive effect whereby the mass loss rate curve exhibits the combined behaviour of the constituent fuels. Under the VDTF's higher heating rate conditions, there is a contrast in the behaviour between the two coals when co-fired. Only the co-firing involving El Cerrejon suggested an additive behaviour as observed with the TGA tests. This is to be discussed further later in this section.

3.3.2. VDTF testing

A more diverse range of co-firing energy ratios are investigated in the VDTF tests. When biomasses are mixed with Chinacite (an anthracite coal), it can be seen in Fig. 12 that the data plots closely fit power trend-lines. Introducing biomass into the fuel mixture results in a relatively large decrease on the distance to ignition. In all of the cases, the ignition distance lies within the relative ignition distances of the constituent fuels. The change in ignition is most significant for the first 25% (on energy basis) of biomass added, with the Eucalyptus ignition point moving over 150 mm closer to the feeder. For the mixtures with biomass energy contribution at 50% and above, the changes in distance to ignition are incremental whereby the ignition distance shifting by <50 mm in

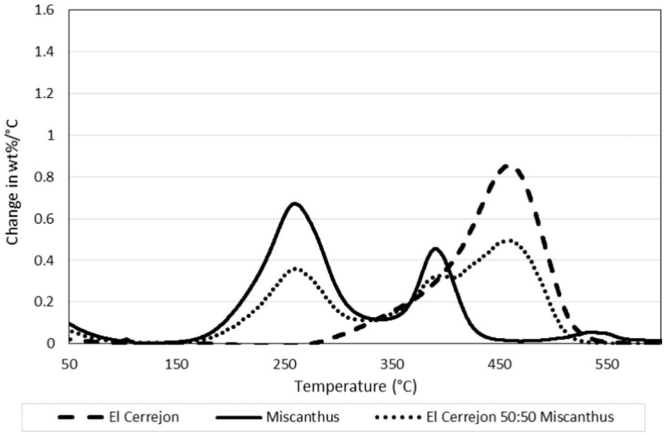

Fig. 11. Mass loss rate comparison of El Cerrejon, Miscanthus and their 50:50 mixture when heated at 3 °C/min in air.

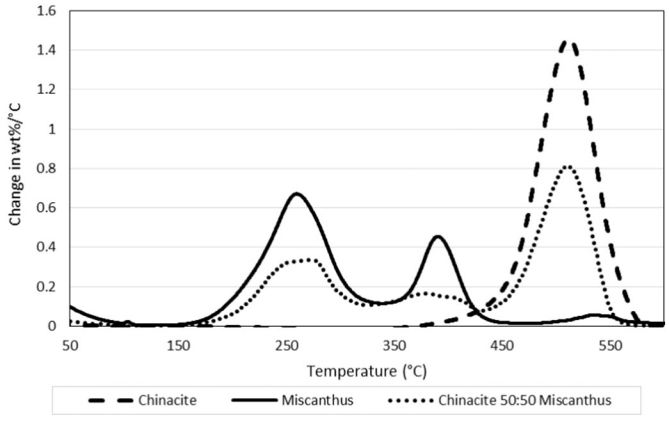

Fig. 10. Mass loss rate comparison of Chinacite, Miscanthus and their 50:50 mixture when heated at 3 °C/min in air.

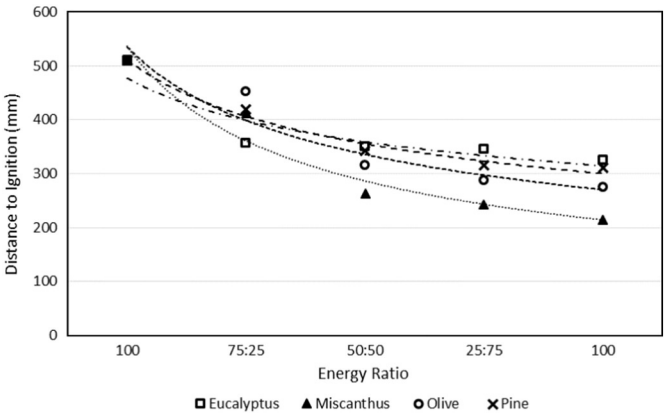

Fig. 12. Chinacite and biomass co-firing ignition performance.

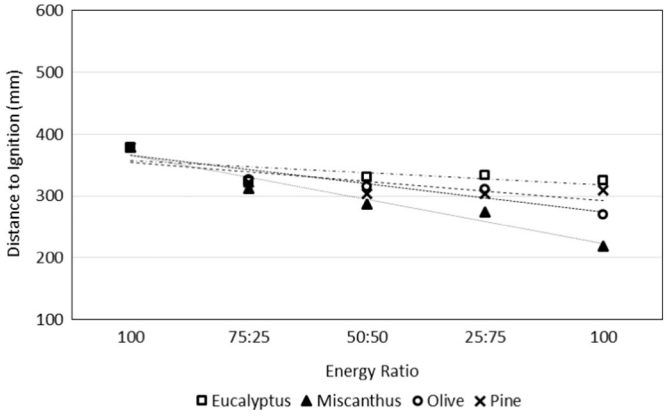

Fig. 13. El-Cerrejon and biomass co-firing ignition performance.

all cases. These are the expected effects of co-firing biomass with unreactive or high rank coals on ignition and combustion as shown by previous studies [9,15,28].

All four tested biomasses can be seen to exhibit similar effects in changing the distance to the ignition of Chinacite and biomass mixtures (Fig. 12), with the Miscanthus, Olive Residue, and Pine showing an almost parallel behaviour. This indicates synergistic and non-additive behaviour from all of the biomass fuels, and relates to previous observations in the reduction of ignition temperatures and delay between volatile and char ignition from co-firing biomass with anthracite by Riaza et al. [29].

When biomasses are mixed in increasing proportions with El Cerrejon which is a bituminous coal (Fig. 13), a diminished influence of biomass addition is observed compared to the anthracite-biomass tests. The distance to ignition still decreases as the proportion of biomass increases, from 373 mm with El Cerrejon coal to 219–324 mm with the 100% biomass. The trend lines R^2 values are high (>0.84) with the exception of coal-Eucalyptus co-firing, which is mainly due to the distance to ignition for coal-Eucalyptus mixtures remaining almost constant regardless of increasing beyond 25% biomass.

The results from the anthracite and bituminous coal co-firing correspond with the findings by Wang et al. [30] which were based on TGA testing only. Their observations are comparable to the thermogravimetric burnout and VDTF test results of this study. Wang et al. [30] concluded that co-firing biomass with anthracite showed a more significant positive synergistic effect on ignition compared to co-firing with bituminous coal. It was also noted that woody biomass did not have as much effect as the straw in their co-firing tests. The Miscanthus co-firing results in this study displayed a similar behaviour whereby a more notable impact on ignition was seen in comparison with the woody fuels tested.

In contrast to the anthracite and bituminous coals, the lignite has a more similar volatile content to that in the biomasses, and as shown in Fig. 14, there are no significant changes on ignition distance at different blend ratios. This is not surprising as the lignite, which had a quite low moisture content (8.2%, Table 1) when it was tested in the VDTF, has a distance to ignition similar to that of biomass. The effect of fuel moisture content on ignition distance was investigated in a parallel set of tests with pine particles [31] using the same VDTF and high-speed camera. The results of these tests, not being included in this paper, clearly show that increasing the moisture level increases the ignition distance and decreases the flame intensity and size. This agrees with the findings of Ma et al. [32] who found it took 3.5 times longer to reach ignition temperature when the biomass moisture content was elevated to 25 wt% from 5 wt%.

To find the correlation between the combined fuel volatile matter content and the distance to ignition of the co-firing fuels, the volatile matter content of the co-firing fuels was calculated from the weight percentage of each fuel in the mixture, as originally determined from the HHV content of each fuel and its proximate volatile matter content. It is well known that the volatile yield of a solid fuel at high temperatures and high heating rates is higher than that of the proximate volatile matter [33,34]. Nevertheless, the calculated proximate volatile matter content is used as a correlation parameter for the observed ignition distance.

Fig. 15 represents the correlation between Chinacite and each of the biomasses. It can be observed that the co-firing fuel mixture shows an amalgamation of the behaviour seen separately for the coal and biomass ignition studies. On the macro-level, there is a general decrease in the distance to ignition with the volatile matter content, as was observed with the coal ignition. On the relative micro-scale, there is an increase in the distance to ignition with the volatile matter content amongst each of the co-firing energy ratio categories. However, this is only observed when biomass in the mixture is 50% or more.

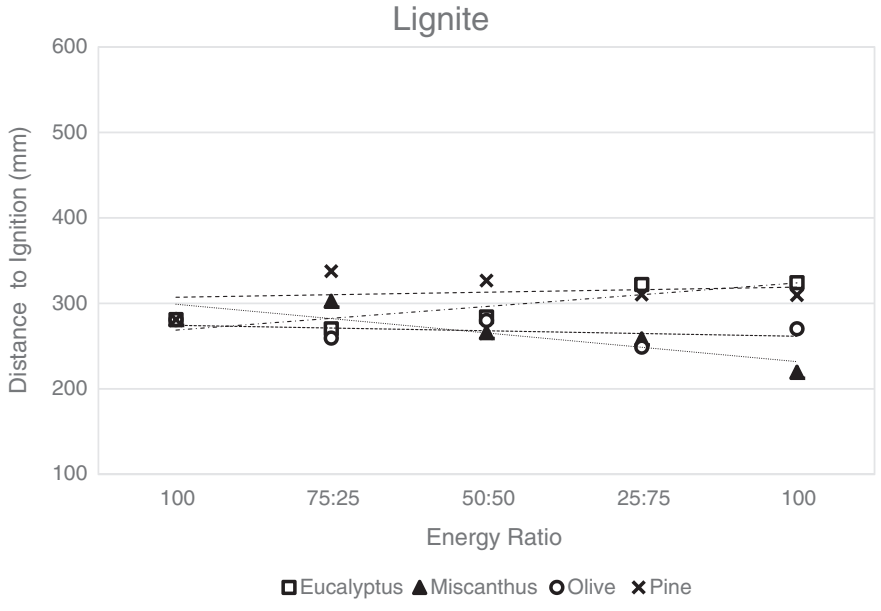

Fig. 14. Lignite and biomass co-firing ignition performance.

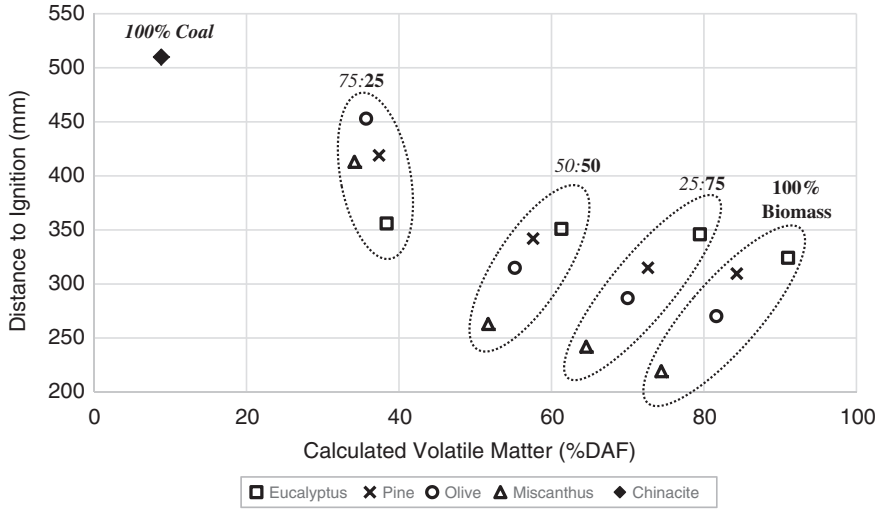

Fig. 15. Relation between the volatile matter content of the co-fired Chinacite-biomass mixtures and the distance to ignition.

In the El Cerrejon co-firing tests, as shown in Fig. 16, a similar trend is observed; note the change in the volatile matter axis scale. It can be seen in both Fig. 15 and Fig. 16 that with 25% and higher energy ratios of biomass, the change in ignition distance of coal-Eucalyptus mixtures is the smallest compared to the other biomass fuels, and in both cases maintaining an almost constant distance to ignition. Pine and Olive show similar behaviour with a 20–50 mm decrease in the distance to ignition each time the biomass energy ratio is increased by 25%. Miscanthus displays the biggest change after each addition of biomass; after the initial addition of 25% biomass, the distance to ignition of the coal-Miscanthus mixture decreases by a further 200 and 100 mm in the Chinacite and El Cerrejon experiments respectively.

Correlations are more difficult to elucidate for the lignite (Fig. 17) than for the other coals due to the closer proximity of the co-fired fuels' volatile matter contents. The addition of 25% Pine and Miscanthus cause an initial increase in ignition distance, followed by a decrease at higher biomass ratios. The increased variance in ignition behaviour is possibly attributed to the competition for oxygen between the low rank coal and the co-fired biomass, as the biomass would evolve a larger volatile cloud during the early stage of the combustion process [5].

4. Conclusions

The present study has focused on the results obtained when combusting pulverised coal and biomass fuels, both separately and in combination, in a Visual Drop Tube Furnace through which a combustion flame established by continuous fuel feeding was observed and recorded using a high speed camera. The automated image post-processing technique implemented to quantify the results has translated the observed fuel ignition characteristics successfully.

The results of the coal combustion tests have showed that the increase in the distance to ignition are correlated with the decreasing volatile content in the fuel, following the trend of prior research in the area [1,29]. With the biomass combustion tests, it was found that the distance to ignition increases with the volatile matter content in the fuel, an opposite trend to what was observed with the coal tests. The same ranking of biomass fuels by ignition behaviour was also reflected in the TGA combustion tests under slow heating rate conditions (3 °C/min). Further, co-firing biomass to anthracite coal has resulted in a significantly reduced distance to ignition, which follows a power trend-line correlation with the biomass co-firing energy ratio. However, a much

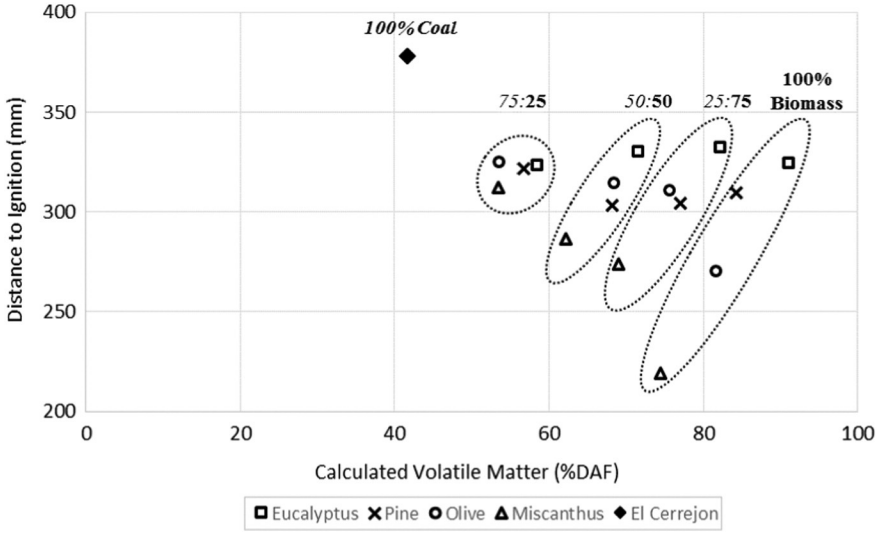

Fig. 16. Relation between the volatile matter content of the co-fired El Cerrejon-biomass mixtures and the distance to ignition.

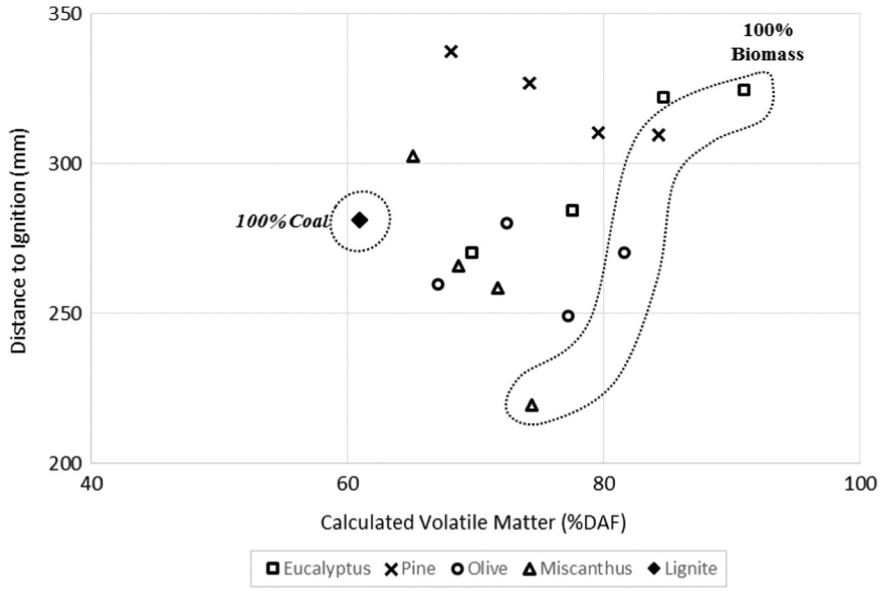

Fig. 17. Relation between the volatile matter content of the co-fired lignite-biomass mixtures and the distance to ignition.

less pronounced effect on the ignition was found when biomass was co-fired with the low to medium rank coals. Co-firing biomass with the bituminous coal showed a limited additive behaviour, whereas co-firing biomass with the lignite displayed similar ignition behaviours at different biomass co-firing ratios.

The difference in the ignition/combustion behaviour between coal, biomass and their mixtures is believed to be related to the different compositions and combustion mechanisms of coal and biomass. The synergistic effect on the ignition of the biomass-anthracite mixture is mainly attributed to the high volatile content and the potential effects of catalysis from the alkali metals present in the biomass [15,16,21,29,30].

From these results of this study, it can be concluded that the VDTF testing coupled with the image analysis technique allows for an effective and simple method of characterising combustion/ignition behaviour of pulverised coal, biomass and their mixtures.

Acknowledgements

This work was supported by the UK Engineering Physical Sciences Research Council (EP/G037345/1); the UK Carbon Capture and Storage Research Centre (EP/K000446/1, EP/K000446/2, Call 1 Project: C1-27); Doosan Babcock Ltd. and Scottish and Southern plc. (SSE).

References

[1] R. Khatami, Y. Levendis, An overview of coal rank influence on ignition and combustion phenomena at the particle level, Combustion and Flame 164 (2016) 22–34.
[2] Y. Levendis, K. Joshi, R. Khatami, A.F. Sarofim, Combustion behavior in air of single particles from three different coal ranks and from sugarcane bagasse, Combust Flame 8 (2011) 452–465.
[3] L.A. Zhang, E. Binner, B. Sankar, High-Speed Camera Observation of a Bituminous Coal Combustion in Air and O_2/CO_2 Mixtures and Particle Velocity Measurement, 26th Annu. Int. Pittsburgh Coal ConfCurran Associates, Inc., New York, NY 2009, pp. 659–669.
[4] J. Matthes, J. Hock, P. Waibel, A. Scherrmann, H.-J. Gehrmann, H.B. Keller, A high-speed camera based approach for the on-line analysis of particles in multi-fuel burner flames, Experimental Thermal and Fluids Science 73 (2016) 10–17.
[5] J. Riaza, L. Alvarez, M. Gil, R. Khatami, Y. Levendis, J. Pis, C. Pevida, F. Rubiera, Ignition behaviour of coal and biomass blends under oxy-firing conditions with steam additions, Green House Gases 3 (5) (2013) 397–414.
[6] E. Marek, B. Świątkowski, Experimental studies of single particle combustion in air and different oxy-fuel atmospheres, Appl. Therm. Eng. 66 (2014) 35–42.
[7] S. Su, J. Pohl, D. Holcombe, J. Hart, Techniques to determine ignition, flame stability and burnout of blended coals in p.f. power station boilers, Prog. Energy Combust. Sci. 27 (2001) 75–98.
[8] P. Molcan, G. Lu, B.T. Le, Y. Yan, B. Taupin, S. Caillat, Characterisation of biomass and coal co-firing on a 3MWth combustion test facility using flame imaging and gas/ash sampling techniques, Fuel 88 (2009) 2328–2334.
[9] A. Gonzalez-Cencerrado, B. Peña, A. Gil, Experimental analysis of biomass co-firing in a pulverized swirl burner using a CCD based visualization system, Fuel Process. Technol. 130 (2015) 299–310.
[10] Y. Levendis, A. Atal, B. Courtemanche, J. Carlson, Burning characteristics and gaseous/solid emissions of blends of pulverized coal with waste tire-derived fuel, Combust. Sci. Technol. 131 (1998) 147–185.
[11] J.M. Jones, A. Saddawi, B. Dooley, E.J.S. Mitchell, J. Wemer, D.J. Waldron, S. Weatherstone, A. Williams, Low temperature ignition of biomass, Fuel Process. Technol. 134 (2015) 372–377.
[12] W. van de Kamp, D.J. Morgan, The Co-firing of pulverised bituminous coals with straw, waste paper, and municipal sewage sludge, Combust. Sci. Technol. 121 (1996) 317–332.
[13] E. Ozgur, S. Miller, B. Miller, M. Versan Kok, Thermal analysis of co-firing of oil shale and biomass fuels, Oil Shale 29 (2) (2012) 190–201.
[14] M. Varol, A.T. Atimtay, B. Bay, H. Olgun, Investigation of co-combustion characteristics of low quality lignite coals and biomass with thermogravimetric analysis, Thermochim. Acta 510 (2010) 195–201.
[15] C. Moon, Y. Sung, S. Ahn, T. Kim, G. Choi, D. Kim, Effect of blending ratio on combustion performance in blends of biomass and coals of different ranks, Exp. Thermal Fluid Sci. 47 (2013) 232–240.
[16] T. Farrow, C. Sun, C. Snape, Impact of biomass char on coal char burn-out under air and oxy-fuel conditions, Fuel 114 (2013) 128–134.
[17] Vision Research, Phantom v12.1 Data Sheet, Wayne, NJ, Vision Research, 2012.
[18] N. Otsu, A threshold selection method from gray-level histograms, IEEE Transactions on Systems, Man, and Cybernetics 9 (1) (1979) 62–66.
[19] J. Chen, Q. Bao, Digital image processing based fire flame color and oscillation frequency analysis, Elsevier, Procedia Engineering 45 (2012) 595–601.
[20] T. Grotkjær, K. Dam-Johansen, A.D. Jensen, P. Glarborg, An experimental study of biomass ignition, Fuel 82 (2003) 825–833.
[21] Saddawi, A. and Jones, J. M. and Williams, A. and Nowakowski, D. J. "Behaviour and Role of Alkali Metals in Biomass Combustion". Conference on Biomass, Bioenergy and Biofuels (21–23 September 2010, Birmingham, UK)
[22] L. Darvell, J.M. Jones, I. Shield, N. Yates, A. Riche, T. Barraclough, The influence of agronomic treatment on the combustion characteristics of some energy crops, Biomass Energy Crop. III Asp. Appl. Biol. (2008) 269–276.
[23] M.E. Fuentes, D.J. Nowakowski, M.L. Kubacki, J.M. Cove, T.G. Bridgeman, J.M. Jones, Survey of influence of biomass mineral matter in thermochemical conversion of short rotation willow coppice, J. Energy Inst. 81 (2008) 234–241.
[24] C. Zhou, G. Liu, X. Wang, C. Qi, Co-combustion of bituminous coal and biomass fuel blends: thermochemical characterization, potential utilization and environmental advantage, Bioresour. Technol. 218 (2016) 418–427.
[25] J. Li, M. Paul, K. Czajka, Studies of ignition behavior of biomass particles in a downfire reactor for improving Co-firing performance, Energy Fuel 30 (2016) 5870–5877.
[26] R. Weber, Y. Poyraz, A.M. Backmann, S. Brinker, Combustion of biomass in jet flames, Proc. Combust. Inst. 35 (2015) 2749–2758.
[27] T.D. Bennet, Biomass Combustion and Ash Behaviour Relating to Pulverised Fuel Power Plants(Doctor of Engineering Thesis) University of Nottingham, UK, 2015.
[28] A. Gonzalez-Cencerrado, B. Peña, A. Gil, Coal flame characterisation by means of digital image processing in a semi-industrial scale PF swirl burner, Appl. Energy 94 (2012) 375–384.

[29] J. Riaza, R. Khatami, Y. Levendis, et al., Single particle ignition and combustion of anthracite, semi-anthracite and bituminous coals in air and simulated oxy-fuel conditions, Combust. Flame 161 (2014) 1096–1108.
[30] X. Wang, Z. Hu, S. Deng, Y. Wang, B. Wei, H. Tan, Investigation of the synergistic effect of biomass Co-firing in the atmosphere of O_2/CO_2, Journal of Biobased Materials and Bioenergy 8 (2015) 1–8.
[31] A.C. Sarroza, Developing a Computational Fluid Dynamics Model to Predict the Effects of Moisture on Combustion Behaviour(Doctor of Engineering Thesis) University of Nottingham, UK, 2015.
[32] L. Ma, M. Pourkashanian, A. Williams, J.M. Jones, Modelling the combustion of pulverized biomass in an industrial combustion test furnace, Fuel 86 (2007) 1959–1965.
[33] G.M. Kimber, M.D. Gray, Rapid devolatilization of small coal particles, Combust. Flame 11 (1967) 360–362.
[34] J. Johansen, R. Gadsbøll, J. Thomsen, P. Jensen, P. Glarborg, P. Ek, ... R. Mitchell, Devolatilization kinetics of woody biomass at short residence times and high heating rates and peak temperatures, Appl. Energy 162 (2016) 245–256.